**Supplemental Table 1**

Quantification of fluorescence staining results

**Figure 1F**

| | Desmin / CD31 | | PCNA / CD31 | | Calponin / CD31 | |
|---|---|---|---|---|---|---|
| **Co** | **692** | **1.0** | **225** | **1.0** | **994** | **1.0** |
| **co DOCA** | **653** | **0.9** | **659** | **2.9** | **411** | **0.4** |
| **Δ*I*-** | **736** | **1.0** | **331** | **1.0** | **1179** | **1.0** |
| **Δ*I*- DOCA** | **579** | **1.2** | **654** | **2.0** | **260** | **0.2** |

**Figure 4A**

| | p-Myl9 / a-SMA | | p-Myl9 / Desmin | | p-Myl9 / F-actin | | p-Myl9 / F-actin | |
|---|---|---|---|---|---|---|---|---|
| | Retinal arteries | | Mesenteric arteries | | VSMCs | | MEFs | |
| **co** | **0.47** | **1.0** | **1.12** | **1.0** | **0.96** | **1.0** | **1.02** | **1.0** |
| **Δ*I*-** | **0.18** | **0.38** | **0.12** | **0.11** | **0.45** | **0.47** | **0.35** | **0.34** |

**Supplemental Figure 1**

| | Myl9 / CD31 | | p-Myl9 / CD31 | |
|---|---|---|---|---|
| **co** | **1182** | **1.0** | **1305** | **1.0** |
| **co DOCA** | **1144** | **0.96** | **1278** | **0.98** |
| **Δ*I*-** | **251** | **0.21** | **339** | **0.26** |
| **Δ*I*- DOCA** | **566** | **0.48** | **666** | **0.51** |

Raw data presented in black are given as arbitrary units. In addition in red color, fold activation versus sham-operated control animals or versus control (Figure 4) is provided.

**Licht et al., Supplemental Figure 1**

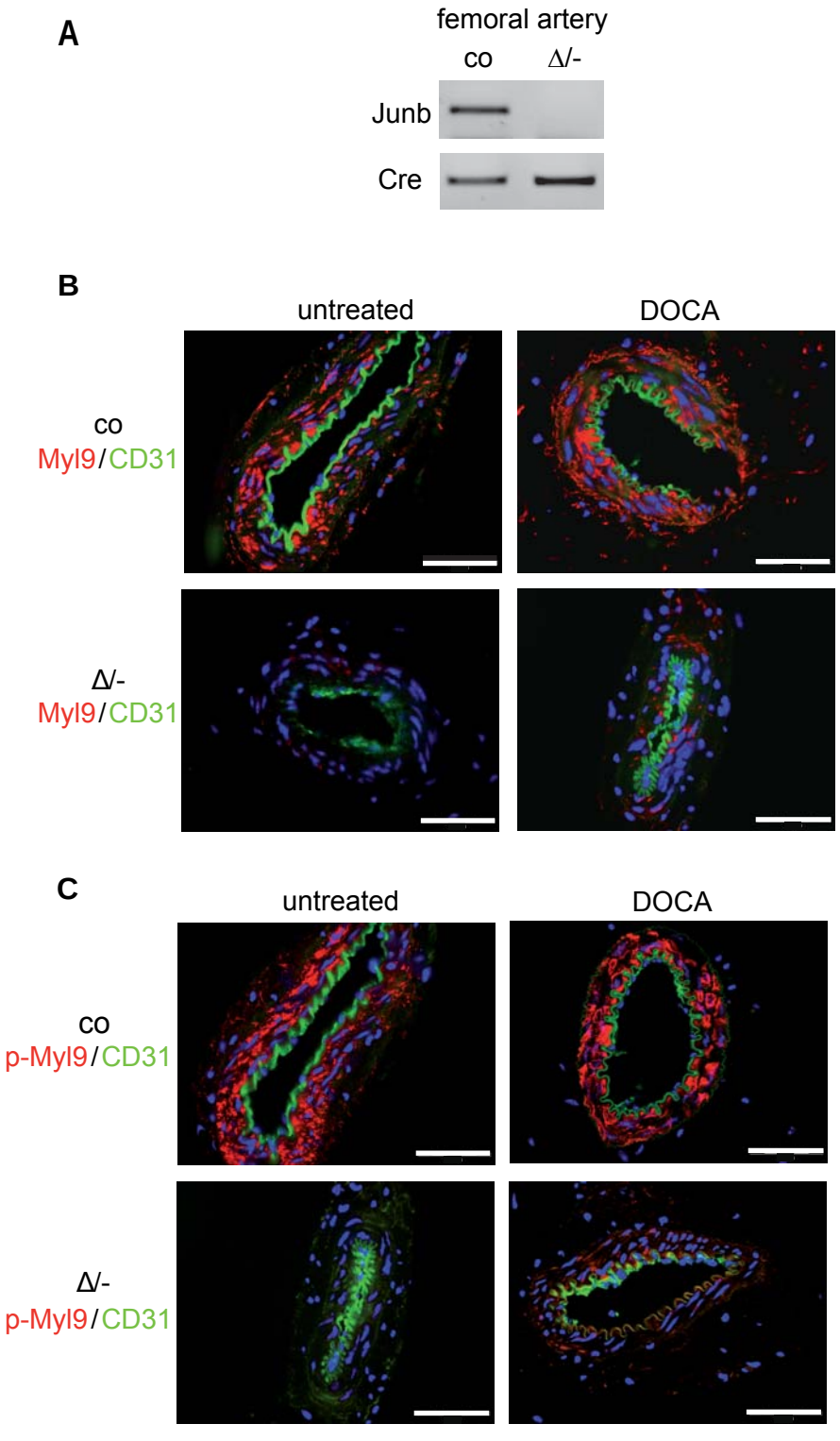

**Licht et al., Supplemental Figure 2**

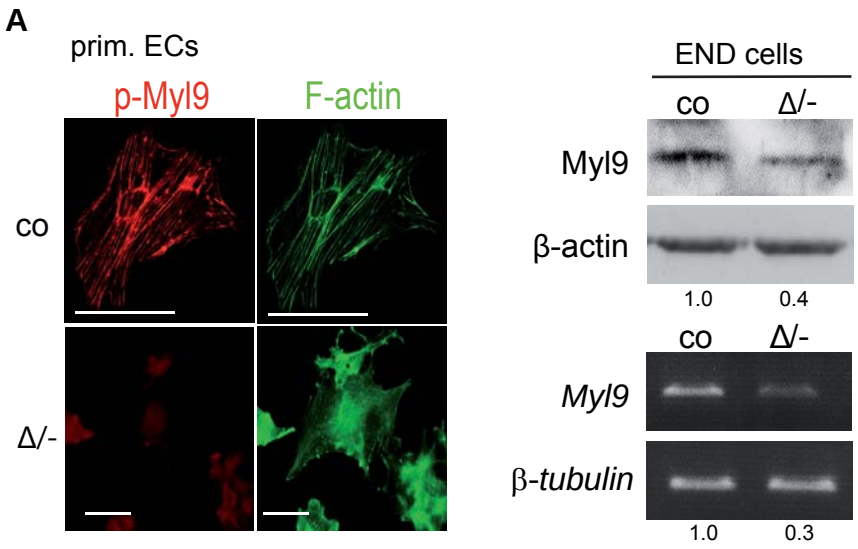


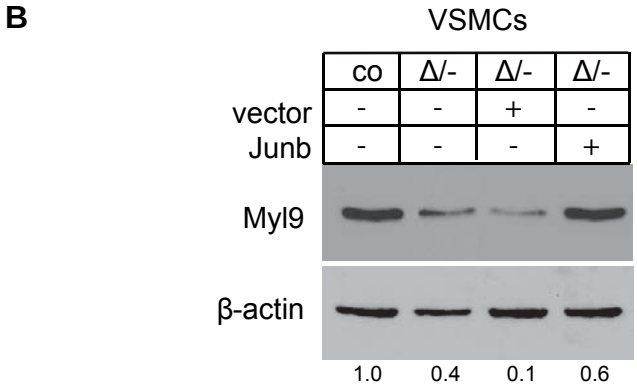


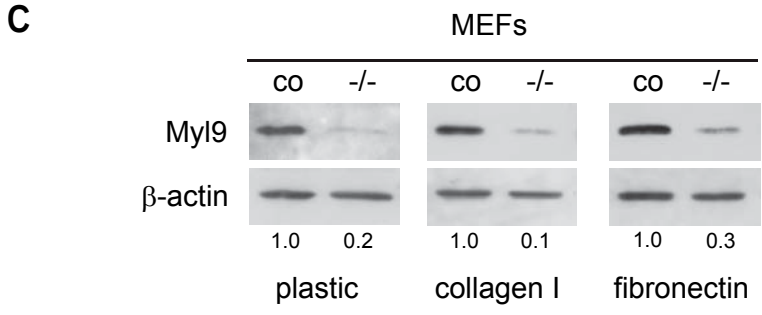

**Licht et al., revised Supplemental Figure 3**

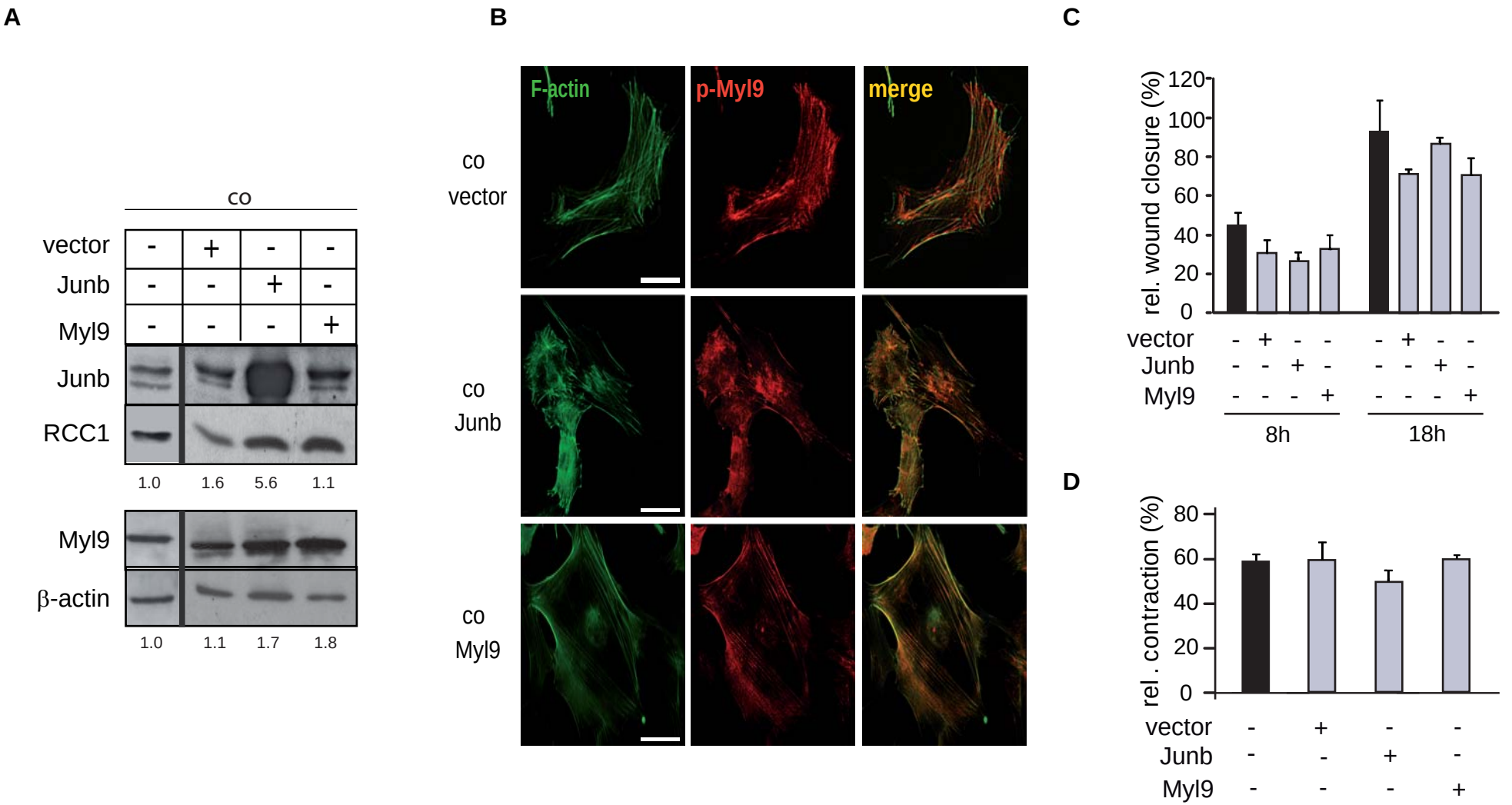

**Licht et al., revised Supplemental Figure 4**

**A**

co

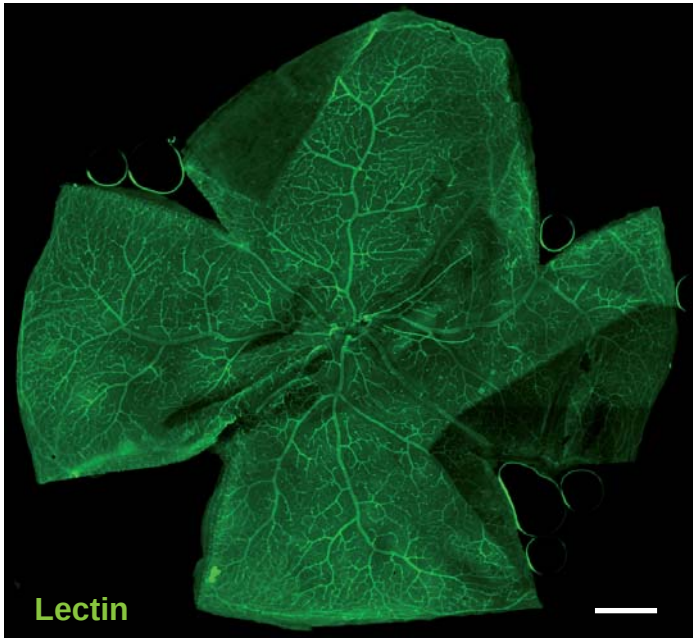


**B**

Δ/-

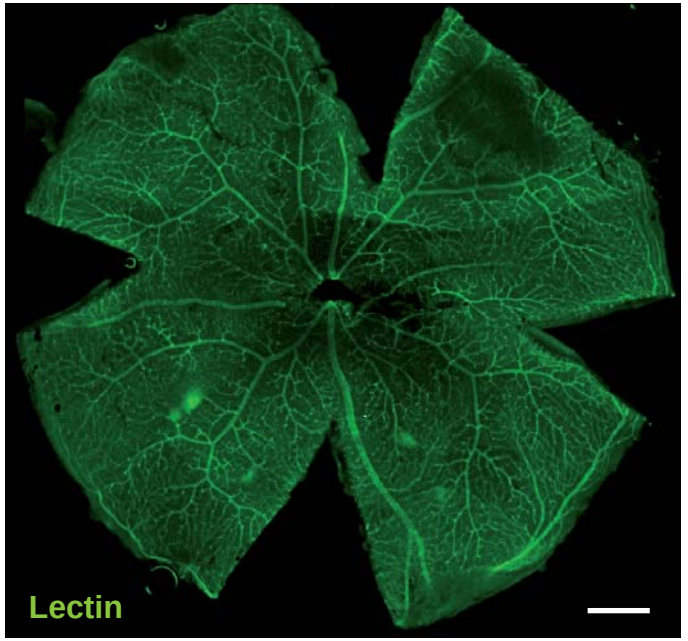

**Supplementary Legends for Licht et al.**

**Supplemental Figure 1**

Hypertension-induced expression and phosphorylation of Myl9 depends on Junb expression. (**A**) Complete deletion of the *Junb* locus was verified by PCR with genomic DNA preparations from femoral arteries isolated from wildtype (co) and Junb-deficient (Δ/-) mice using specific primers. PCR analyses of col1α2-Cre (Cre) served as a control for equal quality and loading. (**B, C**) Immunofluorescence co-staining of femoral arteries isolated from DOCA-salt-treated control (co) and $Junb^{\Delta/-}$ (Δ/-) mice or untreated animals for Myl9 (B), phosphorylated Myl9 (C) and CD31 (green) as indicated (B, C). Size bars correspond to 50 $\mu$m. In each case one representative staining of sections of at least 3 different mice is shown ($n \geq 3$).

**Supplemental Figure 2**

(**A**) Left, levels of phosphorylated Myl9 were assessed by immunofluorescence staining with a specific antibody recognizing phospho-Ser-19 of Myl9 (p-Myl9) in control (co) and $Junb^{\Delta/-}$ (Δ/-) primary endothelial cells (EC). EC were co-stained with phalloidin-Alexa 488 (green) to visualize stress fibers. Size bars correspond to 10 $\mu$m. Right top, immunoblot analysis reveals diminished Myl9 protein levels in $Junb^{\Delta/-}$ endothelioma cells (END cells) (Δ/-). β-actin served as a control for equal quality and loading. Right bottom, semi-quantitative RT-PCR analysis confirms reduced expression of Myl9 in $Junb^{\Delta/-}$ (Δ/-) END cells on mRNA level. *β-tubulin* served as a control for equal quality and loading. (**B**) Re-expression of Junb upon retroviral transduction of $Junb^{\Delta/-}$ (Δ/-) VSMCs restores Myl9 protein levels as shown by immunoblot analysis. (**C**) Immunoblot analysis reveals diminished Myl9 protein expression levels in $Junb^{-/-}$ MEFs (-/-) independent of extracellular matrix composition (plate coating) as indicated. (**B**, **C**) β-actin served as a control for equal quality and loading of 50 $\mu$g total cell extracts. (**A**, **B**,

**C**) Results of densitometric quantification of blots are indicated under each lane. In each case one representative result of 3 different cell preparations is shown (n = 3).

**Supplemental Figure 3**

Overexpression of Junb or Myl9 in wild-type MEFs has no impact on stress fiber formation, cellular motility and contraction capability. (**A**) Overexpression of Junb or Myl9 was confirmed by immunoblot analysis of nuclear (Junb) and total (Myl9) extracts from untreated (co) or retrovirally transduced MEFs. Transduction of the empty vector served as control. RCC1 and β-actin served as control for equal quality and loading. Results of densitometric quantification of blots are given below each lane. One representative result of 3 independent cell preparations is shown (n = 3). (**B**) Immunofluorescence staining for F-actin and phosphorylated Myl9 (p-Myl9) of wild-type MEFs (co) transduced with an empty, Junb- or Myl9-encoding retroviral expression vector. Size bars correspond to 10 $\mu$m. One representative staining of at least 3 independent experiments is shown (n ≥ 3). (**C**) Top, graph displays relative wound closure of wild-type MEFs and of same cells transduced with empty vector, Junb- or Myl9-containing vector subjected to scratch wounding. Values were calculated from images of the wound area taken at zero, eight and eighteen hours post wounding. Error bars represent S.D. values of at least three independent experiments (n ≥ 3). Bottom, graph depicts relative collagen gel contraction by wild-type MEFs transduced with an empty, Junb- or Myl9-encoding retroviral expression vector. Gel contraction capability was determined 96 hours post seeding as percentage of the initial gel surface area that was set to 100 %. Results represent the mean ± SD of 3 independent experiments of quadruplicate gels each (n = 3).

**Supplemental Figure 4**

The retinal microvasculature is normally developed in Junb$^{\Delta/-}$ adult mice when compared to wild-type (co) mice. **(A, B)** Whole mount staining of retinal vessels with FITC-coupled lectin (green). Size bars correspond to 300 μm.